8th U. S. National Combustion Meeting
Organized by the Western States Section of the Combustion Institute
and hosted by the University of Utah
May 19-22, 2013

Autoignition of Ethanol in a Rapid Compression Machine

Gaurav Mittal, Varun Anthony Davies, Bikash Parajuli

Department of Mechanical Engineering
The University of Akron, Akron, OH, 44325

Ethanol is a renewable source of energy and significant attention has been directed to the development of validate chemical kinetic mechanism for this fuel. The experimental data for autoignition of ethanol in the low temperature range at elevated pressures is meager. In order to provide experimental data sets for mechanism validation at such conditions, autoignition of homogeneous ethanol/oxidizer mixtures is investigated in a rapid compression machine. Experiments cover a range of pressures (10- 50 bar), temperatures (800-1000 K) and equivalence ratios of 0.3 and 0.5. Ignition delay data is deduced from the experimental pressure traces. The experiments are modeled using an available detailed chemical kinetic mechanism and compared with the experimental data for ignition delays.

1. Introduction

Ethanol is a renewable source of energy and is used as a neat fuel as well as an octane enhancer and oxygenate in gasoline. Several investigations have focused on studying the chemical kinetics of ethanol. The autoignition of ethanol has been studied in shock tubes mostly at high temperatures and pressures less than 5 bar [1-5]. Only limited studies have been conducted at elevated pressures and temperatures less than 1000 K using shock tube [2,3,6] and RCM [6]. Autoignition at low temperatures is influenced by phenomena that are facility specific. In shock tubes for instance, experiments at low temperatures manifest pressure rise due to shock attenuation. In addition, significant fuel-specific pre-ignition behavior is sometimes noted where ignition is inhomogeneous to begin with, and is followed by a pronounced deflagrative phase, compression of the unburned mixture and the eventual autoignition. In the shock tube study of Fieweger et al. [7], they noted that the pressure increase due to the deflagrative phase was able to shorten the time for the autoigniton of methanol by an order of magnitude at 800K and 40 bar. Given the high sensitivity of induction chemistry to perturbation from shock attenuation and deflagrative phase, it is essential to account for such effects in modeling [8].

By using Schlieren imaging in shock tube, Lee et al. [6] also noted deflagrative behavior in ethanol autoignition. Pressure measurements as well as emission signals showed strong pre-ignition behavior with pressure increasing by more than 100% in some cases before autoignition. Ignition delays reported without any pressure histories can be highly misleading and could lead to misinterpretation of the experimental data at low temperatures. In contrast to the study of Lee et al. [6], Cancino et al. [2] did not report any pre-ignition pressure rise in their shock tube study of ethanol and attempted to refine the chemical kinetic mechanism to mimic the plateau in the ignition

delay profile at low temperatures and attributed this behavior to chemical kinetics and not to the facility effects. Whereas Lee et al. argued that the faster ignition in [2], could have come from inhomogeneous and strong pre-ignition effects.

On the other hand, observed ignition delays in RCM are typically longer than shock tubes due to the effect of post-compression heat loss. The data from RCM, however, is free from the pre-ignition pressure rise that is typical of mild ignition in shock tube, and the post-compression heat loss can be satisfactorily modeled to isolate chemical kinetic effects. Since autoignition of ethanol in RCM has been rarely investigated, the objective of this work is to study the same and provide useful data for mechanism validation and refinements. In the following, experimental facility is first described followed by the results of autoignition experiments and comparison with a kinetic model.

2. Experimental Facility

Except some notable differences, the design of the present RCM is based on [9]. As shown in Fig. 1, the experimental facility is divided into three main components: the pneumatic driving system, the hydraulic system, and the compression and combustion chamber. The pneumatic system consists of a driver cylinder with a bore of 6 inch connected to a 20 gallon air tank. The driver cylinder and the air tank have operating pressures of 250 psi and 200 psi, respectively. The driver cylinder performs two distinct functions. First, it drives the entire piston assembly and prevents its rebound after the end of the compression stroke. Second, it helps retract the piston assembly to its initial position after every run. The hydraulic system consists of a hydraulic chamber, hydraulic piston, pump and lines for filling, draining, and a solenoid release mechanism for running the machine. The stopping of the piston at the end of the compression stroke is achieved by hydraulic damping.

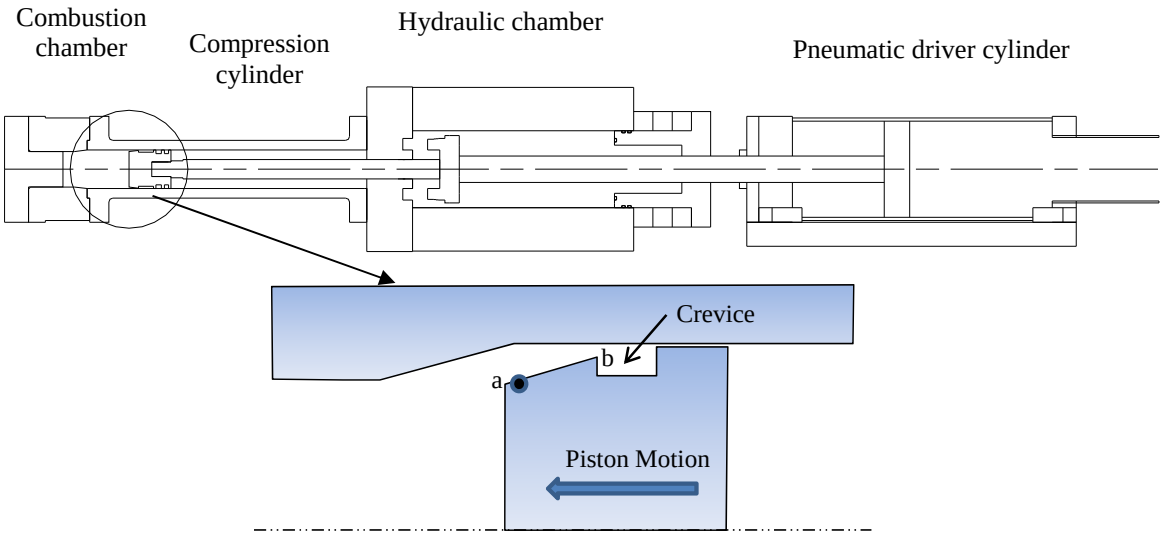

Fig. 1- Schematic of the RCM with crevice containment

The combustion chamber (bore 1.84 inch) is connected to the compression cylinder (bore 2 inch) through a gradually converging section. In addition, the compression piston incorporates a crevice

and a seal on the piston taper surface to enable 'crevice containment', as shown in Fig. 1. The volume of the crevice, the angle of the taper in the reaction chamber and the contraction ratio (defined as the ratio of cylinder diameters on both sides of the taper) were optimized using CFD simulations [10]. The seal on the piston for 'crevice containment' engages only near the end of the compression stroke and separates the main combustion chamber from the crevice during the post compression duration. Therefore, during the compression stroke, the crevice is connected to the main chamber and avoids the formation of the roll-up vortex. Subsequently, during the post-compression period, the crevice and the main reaction chamber are separated to avoid the flow of additional mass into the crevice when chemical heat release takes place in the main chamber. This in turn avoids associated multi-dimensional effects and also improves the fidelity of the zero-dimensional modeling for interpreting experimental data.

The compression stroke can be varied between 8 and 12 inches and the clearance volume is also adjustable allowing a range of compression ratios up to 16. The combustion chamber is equipped with the sensing devices for measuring pressure and temperature, and gas inlet/outlet ports for filling gas. The dynamic pressure during the experiment is measured using a piezoelectric sensor (Kistler 6052C) and a charge amplifier (Kistler 5010B). Further, the pneumatic-hydraulic driving system is designed to allow compressed pressures up to 100 bar and combustion chamber is designed to withstand post-combustion pressures up to 500 bar. The test mixture is first prepared manometrically inside a 5 gallon tank. An Omega absolute pressure sensor (PX409-050AI) is used with the process indicator (DP41-E) for measuring the partial pressures. Before preparing the mixture, the mixing tank is vacuumed using a BOC Edwards RV-5 vacuum pump. After adding individual gases to the mixing tank, the mixture is allowed to homogenize before feeding to the combustion chamber.

Autoignition investigations for ethanol/O_2/N_2/Ar mixtures are conducted over the temperature range of 800–1000 K and the pressure range of 10-50 bar, and for equivalence ratios of 0.3 and 0.5. The mixture compositions are given in Table 1.

Table 1 – Molar composition of test mixtures

#	ϕ	Ethanol	O2	N2	Ar
1	0.3	1	10	8.16	29.44
2	0.5	1	6	1.72	20.84

For a given mixture composition, the compressed gas temperature at the end of compression (top dead center, TDC) is varied by altering the compression ratio, whereas the desired pressure at TDC is obtained by independently varying the initial pressure of the reacting mixture. The temperature at TDC, T_C, is determined by the adiabatic core hypothesis according to the relation $\int_{T_0}^{T_c} \frac{\gamma}{\gamma - 1} \frac{dT}{T} = \ln[P_c / P_0]$, where P_0 is the initial pressure, T_0 the initial temperature, γ is the specific heat ratio that is a function of temperature, and P_C is the measured pressure at TDC.

Numerical modeling of experiments is performed using the Sandia SENKIN code [11] in conjunction with CHEMKIN. The modeling begins from the start of the compression stroke, and includes the effect of heat loss after the end of compression. For each reactive experiment, a non-reactive experiment with a mixture of same specific heat is first conducted. The non-reactive pressure history is used to deduce the effective volume based on adiabatic volume expansion, and

the effective volume is subsequently used to simulate the experiment. Details of the heat transfer modeling approach are similar to those in [9].

3. Results

Figure 2(a) shows an example of pressure trace for autoignition. The measured pressure and the deduced temperature at the end of compression (t=0) are P_C=49.9 bar and T_C=851 K, respectively. It is also seen from Fig. 2(a) that the compression stroke is ~25 ms, and the ignition delay (τ) is defined as the time from the end of the compression stroke, where the pressure peaks at t=0, to the instant of rapid pressure rise due to ignition. Figure 2(b) illustrates an example of the modeling of the same experiment. Experimental and simulated pressure traces for both the reactive mixture and the corresponding nonreactive mixture with the same specific heat ratio are shown in Fig. 2(b). Comparing to the experimental data, the simulated pressure trace for the reactive mixture shows different ignition delay. Therefore, the difference in ignition delay can be used to assess the predictability of the mechanism employed.

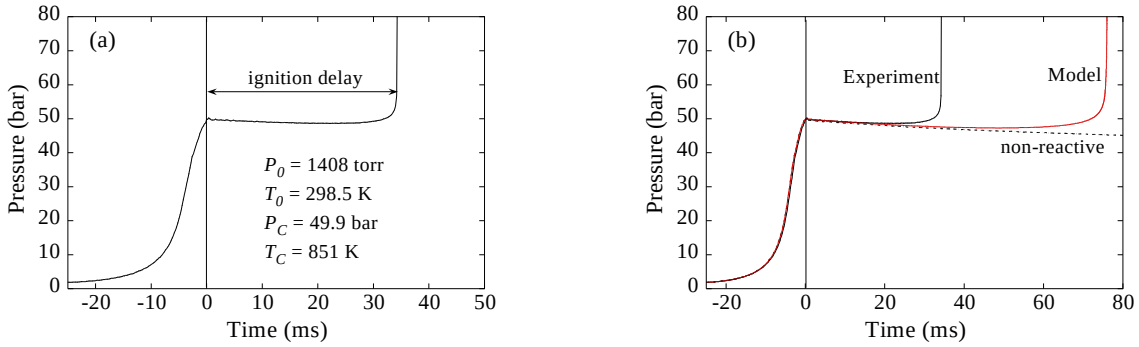

Fig. 2 – (a) Typical experimental pressure traces for ϕ =0.3. (b) Experimental and simulated pressure history. Model used [12]

Figure 3 presents the measured ignition delay times for ϕ = 0.3 at P_C = 10, 25 and 50 bar as a function of the inverse of compressed gas temperature, T_C. A fairly linear variation is seen in this semi-log plot. Pressure dependence of the ignition delay for this Fig. follows $P_C^{-1.63}$. This pressure dependence is, of course, facility dependent due to post-compression heat loss characteristics. Figure 4 presents similar experimental data for ϕ = 0.5 at P_C =10 and 25 bar.

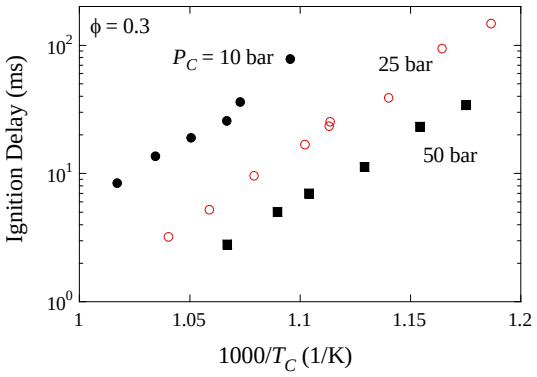

Fig. 3 - Experimental data for ϕ =0.3

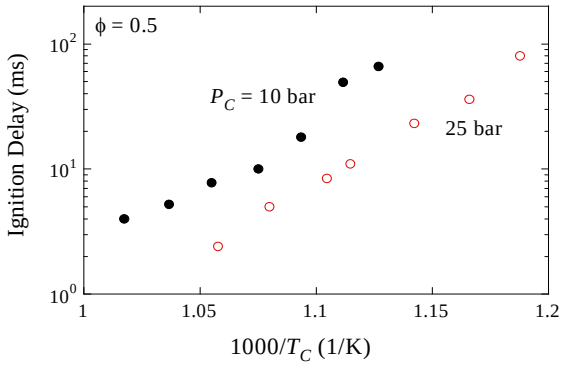

Fig. 4 - Experimental data for ϕ =0.5

Figure 5 shows a comparison of the experimental data with the model of Marinov [12]. At all conditions, an over-prediction from the model is noted. The model of Marinov has been the basis of several other models for ethanol. In due course, more experimental data will be acquired along with comparison with other available kinetic models as well as analysis to identify and resolve the discrepancy between experimental and model results.

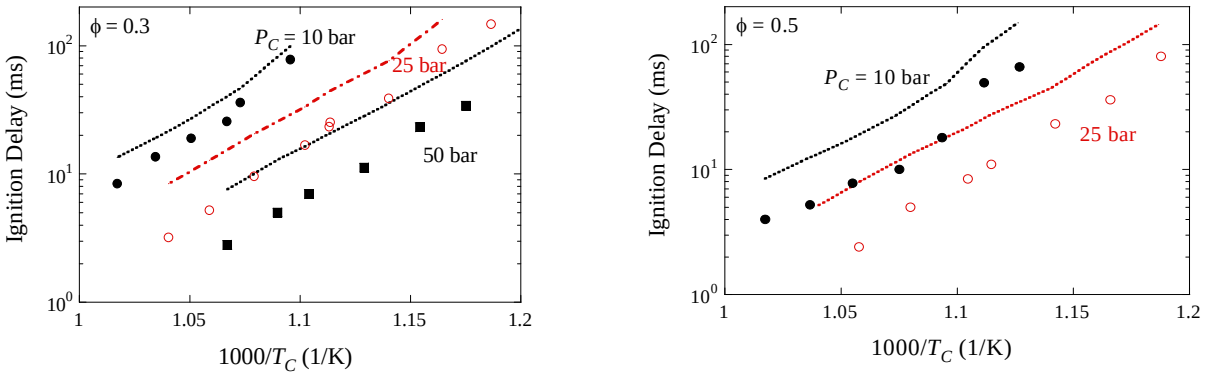

Fig. 5 – Comparison of experimental ignition delays with kinetic model.

References

1. Dunphy, M.P., Simmie, J.M., J. Chem. Soc. Faraday Trans. 87 (1991) 1691.
2. Cancino, L.R., Fikri, M., Oliveira, A.A.M., Schulz, C., Energy Fuels 24 (2010) 2830-2840.
3. Heufer, K., Olivier, H., Shock Waves 20 (2010) 307-316.
4. Curran, H.J., Dunphy, M.P., Simmie, J.M., Westbrook, C.K., Pitz, W.J., Proc. Combust. Inst. 24 (1992) 769.
5. Natarajan, K., Bhaskaran, K.A., Int. Symp. Shock Waves 13 (1981) 834.
6. Lee, C., Vranckx, S., Heufer, K.A., Khomik, S.V., Uygun, Y., Olivier, H., Fernandes, R.X., Z. Phys. Chem. 226 (2012) 1–27.
7. Fieweger, K., Blumenthal, R., Adomeit, G., Combust. Flame 109 (1997) 599-619.
8. Chaos, M., Dryer, F.L., Int. J. Chem. Kin. 42 (2010) 143-150.
9. Mittal, G., Sung, C.J., Combust. Sci. Tech., 2007, 179(3) 497-530.
10. Mittal, G., Gupta, S., Fuel 102 (2012) 536-544.
11. Lutz, A.E., Kee, R.J., Miller, J.A., SENKIN: A FORTRAN Program for Predicting Homogeneous Gas Phase Chemical Kinetics with Sensitivity Analysis. Sandia National Laboratories, Report No. SAND 87-8248, 1988.
12. Marinov, N., Int. J. Chem. Kin. 31 (1999) 183-220.